ELSEVIER

Journal of Nuclear Materials 258–263 (1998) 113–123

journal of nuclear materials

Atomic processes during damage production and defect retention

Nasr M. Ghoniem *

Mechanical and Aerospace Engineering Department, University of California at Los Angeles (UCLA), Los Angeles, CA 90095-1600, USA

Abstract

Fundamental atomic processes during production and retention of radiation damage in structural materials are reviewed. Firmly established damage mechanisms are outlined, and some of the major uncertainties exposed. Damage production under neutron and ion irradiation proceeds through the elementary step of collision cascade formation, with further modification of the nascent cascade structure by inter-, and intra-cascade interaction events. Under fusion neutron irradiation, single cascade damage production occurs within 10 ps in most metals, with spatial extent of several tens to hundreds of nano-meters. Damage accumulation takes place over much longer time and length scales, during which multiple cascades interact leading to further re-structuring of the incipient cascade. Areas which require further investigation are: (1) the mechanisms of vacancy cluster collapse at the cascade core; (2) the athermal nucleation of interstitial loops at the periphery; (3) the migration of interstitial atoms and clusters emanating from the cascade; (4) the replacement of the *dpa* with a more physical measure of damage retention; (5) cascade structure for high PKA energies (above 20 keV); and (6) Inter- and Intra-cascade interactions, (7) and finally, cascade dynamics in damaged materials at high dose.

1. Introduction

Most materials experience significant property changes when irradiated by energetic particles. Plastic yield and subsequent deformation, fracture and dimensional stability of metals and alloys exhibit strong sensitivity to the deleterious effects of neutron irradiation. Electro-optical properties of semi-conductors and insulators are likewise prone to the damaging effects of both ionizing and displacement types of radiation. Extrapolation of the properties of irradiated materials in available damage facilities to those, which might result under the conditions of fusion energy systems, necessitates knowledge of fundamental atomic mechanisms.

In a fusion reactor, energetic neutrons will impart substantial energy to lattice atoms, thus initiating collision cascades and sub-cascades. The initial energy of the Primary Knock on Atom (PKA) is typically six to seven orders of magnitude above its thermal value. This astounding energy density is nevertheless quickly shared amongst neighboring atoms over a short period (on the order of 10 ps for metals), resulting in permanent damage. The initiating event is obviously very violent, and furthermore, is characterized by extremely short time and length scales. Thus, the solid will be driven out of its equilibrium state following this damage production stage.

Although the primary damage event is uncommonly severe, most materials appear to have the capacity of "repairing" themselves. A fraction of the PKA energy is first consumed in heating with no apparent damage. Then, a very small fraction (on the order of a few percent) of the amount of atomic defects will be able to escape the healing power of the cascade zone, and freely migrate in the material. Notwithstanding, the small fraction of freely migrating defects (FMD's) results in substantial modifications of the material's microstructure and hence its properties. In neutron-irradiated materials, damage initially manifests itself as vacancies, interstitials, and their clusters in metals and alloys. In ordered intermetallics and covalently bonded

* Tel.: +1 310 825 4866; fax: +1 310 206 4830; e-mail: ghoniem@ucla.edu.

0022-3115/98/$19.00
PII: S0022-3115(98)00346-8

multi-species materials, additional forms of damage include the formation of anti-site defects, disordering, and amorphous zones.

Atomic re-arrangements and defects produced in the nascent state of the collision cascade can result in many deleterious modifications of the physico-mechanical properties of irradiated materials. However, the long-range migration of FMD's is responsible for the slow, yet permanent evolution of the microstructure. We divide the mechanisms involved in radiation interaction with materials into two broad categories: (1) processes associated with atomic collision phenomena, and (2) processes resulting from diffusive migration of atomic defects. In this paper, we confine our attention to atomic mechanisms in the first category, which may be conveniently termed: damage production and retention. We provide here a brief review of this subject, emphasizing the current firm understanding of some processes, as well as areas where consensus has yet to emerge. Our view is that *production* of atomic defects because of irradiation occurs within the lifetime of a single collision cascade. On the other hand, *accumulation* of damage is viewed to be the consequence of many interacting events, in which both *inter-cascade* and *intra-cascade* interactions are significant.

By the mid 1950s, the two basic concepts of displacement damage production were established. Kinchin and Pease [1] developed the first model for calculating the number of displaced atoms in a solid. No knowledge of the atomic structure is required in this model, and the number of displaced atoms, ν, by a PKA of energy E_{PKA} is readily calculated once the *displacement threshold energy*, E_{d}, is known. Thus: $\nu_{\mathrm{KP}} = E_{\mathrm{PKA}}/2E_{\mathrm{d}}$. Brinkman [2], on the other hand, was the first to propose the *displacement spike* concept, in which the atomic structure was considered. He clearly illustrated the separation between the two types of atomic defects, namely clustered vacancies in the central core of the cascade and interstitial defects on its periphery. Subsequently, Seeger [3] shed considerable light on Brinkman's model, and proposed the ejection of interstitials from the cascade along low-index crystallographic directions in Replacement Collision Sequences (RCS's), and the formation of a *depleted zone* at the cascade center. The production mechanism of stable Frenkel Pairs (FP's), and the number of FP's produced by the PKA were then identified almost half a century ago! Shortly thereafter, Makin and Minter [4] postulated the existence of a volume around each depleted zone within which no new clusters can be formed. Thus, a rudimentary mechanism of damage accumulation and saturation was identified. Intensive experimental and theoretical research during the intervening five decades brought this powerful picture into sharp focus, and modified the quantitative nature of these mechanisms in a substantial way.

2. Fundamental damage mechanisms

2.1. Energy transfer and interatomic potentials

No single interatomic potential function is capable of representing the wide range of energy of displaced atoms. One must therefore resort to a description based on *composite potential* functions. In the high-energy range (i.e. at close separation between nuclei), the Coulomb potential is sufficient. That is: $V(r) = Z_1 Z_2 e^2/r$, where $Z_{1,2}$ are the atomic numbers of interacting atoms, r is their separation distance and e the electronic charge. As the energy decreases, the situation becomes more complex due to the interaction of overlapping electron shells. Atomic collisions above approximately 100–200 eV can be satisfactorily described within the framework of a Binary Collision Approximation (BCA), in which the interatomic potential is a screened form of the pure Coulomb. Below this energy range, several atoms can interact simultaneously, because of the local electronic structure. Since many important features occur in the low energy regime, such as displacement threshold reactions, defect stability and clustering, etc., it is therefore imperative to include *many-body* interactions in defect production calculations. Consequently, estimations of defect production are based on the BCA for the gross features, and on detailed Molecular Dynamics (MD) for a more quantitative analysis. The concept of *displacements per atom (dpa)* is based on the BCA. It utilizes a modified form of the Kinchin–Pease estimate, for the number of displaced atoms per collision.

Energy transfer during atomic collisions is determined by the form of the interatomic potential. In BCA calculations, the potential at separations somewhat smaller than equilibrium is assumed to be represented by the Born–Mayer potential: $V(r) = A\,\exp(-r/\rho)$, where A and ρ are constants. As the separation between the two atoms decreases, a screened Coulomb form is used. The inverse power law potential: $V(r) = Ar^{-s}$, $s = 2,3$, is often used. In this case, exact analytical expressions for the energy transfer cross-section can be readily found, and efficiently used in BCA calculations. The energy transfer cross-section in a collision between the energetic atom (energy E) and the struck atom (emerging with energy T) is analytically given by [5]:

$$\sigma(E,T)\,\mathrm{d}T = C_s E^{-s} T^{-1-s}\,\mathrm{d}T, \tag{1}$$

where C_s is a constant appropriate for the power s. Matching procedures must be used to ensure smooth transitions in energy transfer during BCA energy loss calculations. Alternatively, exponential screening functions can be used to describe the influence of outer shell electrons on diminishing the interaction between nuclei. Ziegler et al. [6] have successfully fitted many atomic scattering experiments with the potential:

$$V(r) = \frac{Z_1 Z_2 e^2}{r} \sum_{k=1}^{4} C_k \mathrm{e}^{-b_k r/a_0}, \tag{2}$$

where C_k and b_k are fitting constants, and a_0 is a screening length.

Stability and final configuration of displaced atoms are properties which are critically dependent on accurate representation of the interatomic potential at energies just around the threshold for displacement (e.g. tens of eV) down to thermal energies (e.g. fractions of eV). Empirical potentials, which are based on equilibrium properties of the solid, are strictly accurate in the fraction of eV range. At higher energies, however, many-body type potentials for low energy interactions are matched with pair potentials [7]. In metals, a widely used potential is the Embedded Atom Method (EAM) function, originally developed by Daw and Baskes [8]:

$$V(r_{ij}) = \phi_{ij}(r_{ij}) + 2\rho_{ij}^{\mathrm{a}} F' + (\rho_{ij}^{\mathrm{a}})^2 F'', \tag{3}$$

where the first term on the right represents repulsive core–core interactions, the second and third are attractive contributions. The embedding function F is assumed to be dependent on the total average electron density around atom i, while the average local electron density contribution from atom j on i are given by ρ_{ij}^{a}. Primes are for derivatives of F. For covalently bonded materials (e.g. SiC or Si), the empirical potential must posses strong directional character. Widely used potentials are the Stillinger–Weber for Si [9], and the Tersoff [10] and Pearson [11] potentials for SiC.

Atomic collisions treated via interatomic potentials lead to energy loss from the PKA, and redistribution to target atoms participating in the collision cascade. However, in-between these collisions, energy is continuously lost from energetic atoms to the electron system in the lattice. The rate of this loss, per target atom per unit area, S_{e}, is described by the Lindhard formula [6] at low energy (below 25 keV/ amu):

$$S_{\mathrm{e}} = 8\pi e^2 a_0 \frac{Z_1^{7/6} Z_2}{Z} \frac{v}{v_0}, \tag{4}$$

where $a_0 = 0.0529$ nm, Z_1 and Z_2 are the charge number for projectile and target, and $Z^{2/3} = Z_1^{2/3} + Z_2^{2/3}$, and v the velocity of the projectile and v_0 is a characteristic electronic speed. In the high energy regime (i.e. PKA energy greater than 200 keV/amu), the Bethe–Bloch stopping power is used:

$$S_{\mathrm{e}} = \frac{2\pi Z_{\mathrm{eff}}^2 e^4 (M_1/m_{\mathrm{e}})}{E} \ln\left(\frac{4E}{(M_1/m_{\mathrm{e}})\bar{I}}\right), \tag{5}$$

where Z_{eff} is an effective charge, M_1 is the projectile mass, m_{e} the electron mass, $\bar{I}$ the average ionization energy of the target atom, and E the PKA energy. In the intermediate energy range of 20–200 keV/amu, the electronic conductance (inverse of S_{e}) as a linear combination of conductances calculated from Eqs. (4) and (5). For polyatomic materials, such as SiC, Al_2O_3, etc., Bragg's additivity rule is used in accordance with the stoichiometry of the compound.

2.2. dpa as a measure of damage accumulation

The concept of "displacements per atom", or simply dpa, has been extensively used as a measure of damage accumulation in irradiated materials. We outline here the procedure for dpa calculations in a multi-species material for generality [11]. Assume that the material is composed of two species, type A and B (e.g. SiC). If a PKA of type A travels a distance dx, it will eventually result in a number of displacements of type A atoms (ν_{AA}), and of type B (ν_{AB}), and similarly for type B PKA. Each element of the matrix ν_{ij} $(i, j = 1, 2)$ is governed by a conservation equation [11]:

$$\begin{aligned}\nu_{ij}(E) = &\sum_k \int_0^{A_{ik}E} \Big\{ \big[\Gamma(E - T - E_{jd}/\Lambda_{ij})\nu_{ij}(E - T) \\ &+ \Gamma(T - E_{kd})(\delta_{kj} + \nu_{kj}(T))\big] N_k \sigma_{ik}(E, T) \Big\} \,\mathrm{d}x \,\mathrm{d}T \\ &+ \int_0^{T_{em}} \nu_{ij}(E - T_e) N_e \sigma_{ie}(E, T) \,\mathrm{d}x \,\mathrm{d}T \\ &+ \left(1 - \sum_k N_k \sigma_{ik}(E) \,\mathrm{d}x - N_e \sigma_{ie}(E) \,\mathrm{d}x\right) \nu_{ij}(E).\end{aligned} \tag{6}$$

In Eq. (6), $\Gamma(x)$ is the unit step function, N_i the atomic density of species i, $\sigma_{ij}(E)$ the total scattering cross-section between i and j, $\Lambda_{ij} = 4m_i m_j/(m_i + m_j)^2$ is the energy transfer efficiency between masses m_i and m_j, and δ_{ij} is the Kronecker delta. The first integral represents the number of displacements ν_{ij} conserved over the probability of a PKA of type i colliding with target atoms $k (k = 1, 2)$ during its travel a distance dx. It has two terms; the displacements caused by the PKA and those caused by the secondary knock-on. The second integral represents the additional displacements conserved over the probability of PKA collisions with electrons. The last term in parentheses on the right is for conservation of displacements over the probability of collisions with neither atoms nor electrons.

Solution of Eq. (6) depends on assumptions regarding the energy transfer cross-section (hence the interatomic potential), as well as the form of electronic energy loss. For the case of a single element material, with no electronic energy loss, and a hard-sphere interatomic potential, the Kinchin–Pease estimate, ν_{KP}, is obtained. It is naturally expected to be too high. If a "softer potential" is used, for example the inverse power law for which the differential energy transfer cross-section is given by Eq. (1), this number is reduced by a factor

$K = 0.5$–1.0, depending on the potential. An acceptable value for K is 0.8, and is due to Norgett, Robinson and Torrens (NRT) [12]. In addition, when the energy loss to electrons is accounted for, the number of displaced atoms is reduced even further. It takes the form:

$$\nu_{\mathrm{NRT}}(E) = K\xi(E)\nu_{\mathrm{KP}}(E), \tag{7}$$

where the factor K is defined as the *displacement efficiency*, and the function $\xi(E)$ is defined as the *damage efficiency*, and are both less than unity.

In a neutron flux described by a differential spectrum $\phi(E_{\mathrm{n}})\,\mathrm{d}E_{\mathrm{n}}$, the differential energy transfer cross-section from a neutron, energy E_{n}, to a PKA, energy E, is $\sigma_{\mathrm{n}}(E_{\mathrm{n}}, E)\,\mathrm{d}E$. The *displacement cross-section*, σ_{d}, can be conveniently defined as: $\sigma_{\mathrm{d}}(E_{\mathrm{n}}) = \int_{E_{\mathrm{d}}}^{\Lambda E_{\mathrm{n}}} \sigma_{\mathrm{n}}(E_{\mathrm{n}}, E)\nu(E)\,\mathrm{d}E$. The displacement rate, in units of *dpa*, is obtained by integration over the neutron spectrum:

$$R_{\mathrm{d}} = \int_{E_{\mathrm{d}}/\Lambda}^{\infty} \sigma_{\mathrm{d}}(E_{\mathrm{n}})\phi(E_{\mathrm{n}})\,\mathrm{d}E_{\mathrm{n}}. \tag{8}$$

Current damage correlations for materials behavior in one type of neutron spectrum (e.g. fission) to another (e.g. fusion) are based on Eq. (8). Fig. 1 shows calculated dpa cross-sections for Fe, C (in SiC), Si (in SiC) and SiC. The cross-sections are up to several thousand barns, and are very dependent on the neutron energy. Because of a smaller E_{d} for C in SiC, the dpa cross-section for C is about four times higher than Si for fusion neutrons [11].

Damage calculation procedure outlined above is overly simplistic for a number of reasons. The actual value of ν, obviously the basis of dpa is highly uncertain because the theory ignores immediate re-structuring of the lattice – the "repair" mechanisms we referred to earlier. As much as 99% restoration of displacements can occur over several time scales!

3. Atomic structure of primary damage

Current experimental techniques do not have access to real-time details of cascade events. For this reason, computer simulations have helped to resolve the atomic structure of collision cascades. The gross features of large-scale cascades can be studied by the Monte Carlo (MC) technique, and involve the utilization of Eqs. (1)–(5) in defining probabilities of interactions and magnitudes of energy transfer. These simulations are based on the BCA; the primary examples are the computer codes MARLOWE [12], TRIM [6] and TRIPOS [5]. The power of MC cascade analysis stems from the fact that

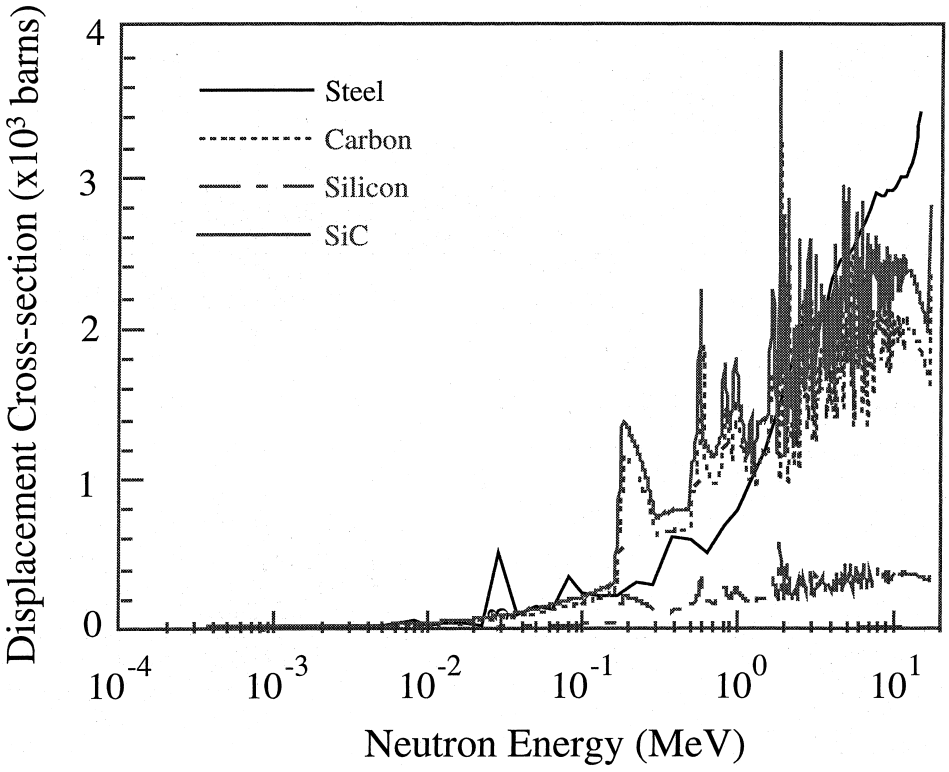

Fig. 1. Displacement cross-sections, as function of neutron energy for Si (in SiC), C (in SiC), SiC, and Fe [11].

large crystal volumes can be simulated, allowing study of high-energy interactions (up to 0.5 MeV). When an *assumed* recombination distance of 5.75 lattice parameters is invoked in subsequent annealing simulations, the surviving defect fraction is shown to be consistent with resistivity measurements for Cu [13].

Experimentally, on the other hand, postmortem or in situ observations of vacancy clusters in metals, alloy disordering of ordered alloys, and amorphous zones in covalent materials can reveal what happened *after* the cascade formation stage. One of the main discrepancies between MC simulations of single cascades and experiments is on the number of sub-cascades that result from the breakup of a single high-energy cascade. Based on spectral analysis of the primary recoils in several metals, Kiritani and coworkers [14] determined the number of sub-cascades as a function of PKA energy. Heinisch [13], and Heinisch and Singh [13] performed MC simulations for single high-energy cascades for Cu, and showed that above 30–50 keV the cascade breaks up into a chain of multiple damage zones. Computer simulation results show a factor of two less sub-cascades as compared to those inferred from experiments, as shown in Fig. 2. What complicates the single cascade picture, and is perhaps responsible for some of this disagreement, is the influence of subsequent cascades on the stability of vacancy clusters [15]. Experimental work on thin foils of Cu, Au and Ni irradiated by 14 MeV neutrons show that, at least at low neutron dose, subsequent cascades tend to aid in collapsing vacancy clusters. This behavior has been interpreted by Kiritani as an *impact effect*, where the phonon energy released from one cascade is transmitted through the lattice to a neighboring one. The elastic energy is thought to collapse the vacancy cluster, because it is found that several cascades are required before a vacancy loop can be observed [14]. Cooperative cascade interactions, as manifest through the impact effect, appear to contradict MD simulations of single cascades, and the "cascade overlap" concept used to explain damage saturation at high neutron doses. Another problem in sub-cascade analysis exists at high temperature, particularly in high Z elements (e.g. Au and Ag) [16]. While experimental evidence indicates that closely-spaced sub-cascades tend to agglomerate and form one contiguous vacancy cluster [14], no theoretical or computational evidence exist to date on either the "impact effect" nor large contiguous vacancy clusters.

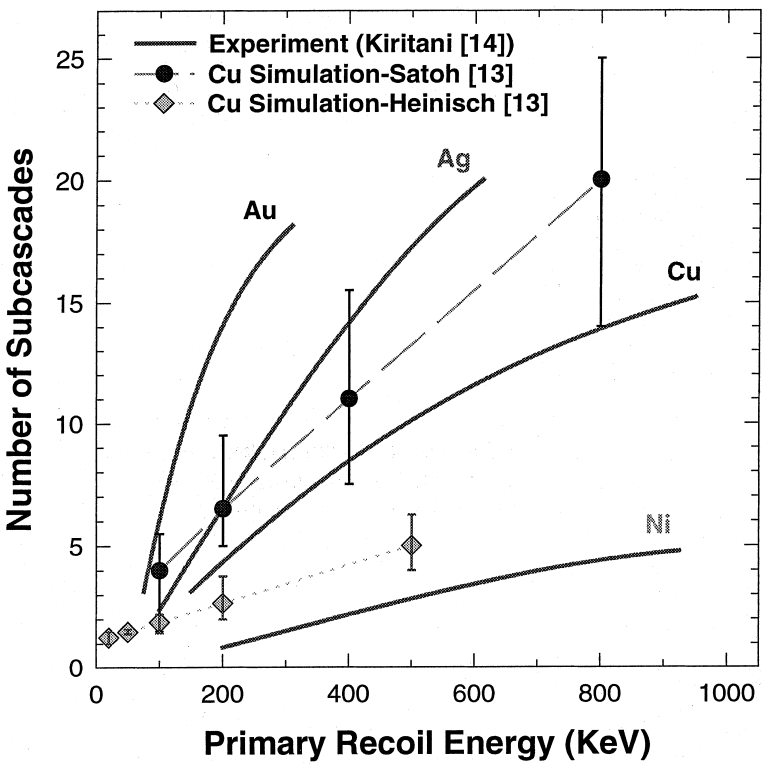

Fig. 2. Dependence of the number of sub-cascades on PKA energy in various elements. Experimental estimates are by Kiritani [14], and computer simulations are by Heinisch [13], and Satoh [13].

3.1. MD methodology

MD simulations are based on direct solution for the equations of motion (EOM) for a large number of atoms. In principle, the interatomic potential is all what is needed, and classical Newtonian mechanics should be sufficient. However, many computational details must be worked out because of the finite size of the system of particles, and the discreteness of numerical integration. The classical EOM are given by [17]:

$$m_i \frac{\partial^2}{\partial t^2}\mathbf{r}_i = -\sum_{j,j\neq i}^{N} \nabla \Phi_{ij} - \mu \frac{\partial}{\partial t}\mathbf{r}_i - k(\mathbf{r}_i - \mathbf{r}_{ie}) + F_{ib} + \eta(t). \tag{9}$$

Integration of Eq. (9) for the atomic position vectors, $\mathbf{r}_i$, is typically done with very short time steps (0.01–1 fs) for accurate trajectories. The atom inertia force on the left side is balanced by the gradient of the interatomic potential, an effective electronic energy loss (friction) force, a net balancing force (F_{ib}) for coupling of the atomic box with the elastic continuum, and a stochastic force ($\eta(t)$) to restore thermodynamic equilibrium with the surrounding medium. Typical calculations for Si on the T3D-MPP computer at LLNL require 2 s/million atoms for each time step [16].

3.2. Displacement threshold

In metals, the production mechanism of a stable Frenkel Pair has been established to be the Replacement Collision Sequence (RCS) [5]. Atoms receiving energy just above the displacement threshold initiate a supersonic RCS, which terminates by displacing one atom at the end of the chain. Consequently, energetic atoms directed along principal cubic directions in the FCC lattice (i.e. $\langle 1\ 1\ 0\rangle$ and $\langle 1\ 0\ 0\rangle$) are easier to displace because of the focusing effect. In open directions, such as $\langle 1\ 1\ 1\rangle$, an energetic atom emanating from a corner must squeeze through a triangle made up of face atoms. MD calculations of E_d in Cu at 10 K compare well with the experimental data of King and Benedek [7]. In Cu, E_d along $\langle 1\ 1\ 0\rangle$ or $\langle 1\ 0\ 0\rangle$ is on the order of 25 eV, while it is almost twice as large close to the $\langle 1\ 1\ 1\rangle$ direction. Similar results have been recently obtained for Fe [16]. MD calculations indicate that the lattice temperature has a significant effect on the length of the RCS in Cu, where it decreases from 6.5 lattice constants to only 3 at temperatures below melting [7].

In covalently bonded materials, the displacement process is more complex, especially when two different atomic species are bonded. Fig. 3(a) shows two primitive tetrahedral unit cells of SiC, while Fig. 3(b) give the results of MD calculations for the displacement threshold surfaces in SiC. Starting from a C atom in the center of the tetrahedron, the vertices and the face centers are both [1 1 1] directions, but for clarity, we will denote the face centers as [1 1 1] while the vertices as $[1\ 1\ \bar{1}]$. It is shown that displacements of C or Si atoms occur at low energies in directions close to the [1 1 1]-gaps, while they require substantially more energy to be displaced along the bond directions (i.e. $[1\ 1\ \bar{1}]$). If an energetic atom is ejected along the direction of its neighbor, it will get reflected and then will be displaced through the opposite [1 1 1]-gap. Stable displaced atoms (interstitials) then reside on $\{1\ 1\ 1\}$ planes within the neighboring primitive cell, known as hexagonal (or H-) sites. In contrast to metals, it appears that displacement damage in covalent materials does not require the large separation of Frenkel Pairs via the RCS mechanism. The low displacement threshold of C as compared to Si indicates that displaced atoms will predominantly be of the C-type. If a Si atom is ejected through the [1 1 1]-gap bounded by a triplet of C atoms, it will displace the entire triplet on its way. Not only that C is displaced at a lower threshold, but it is also simultaneously displaced whenever a Si displacement occurs.

3.3. Collision cascade features

In metals, computer simulations reveal that high local temperatures and local melting occur at the cascade core, followed by solidification because of energy conduction away from its center. Temperature gradients as high as 10^{10} K/cm, and cooling rates of 10^{15} K/s have been estimated for 25 keV cascades [16] in Cu. The cascade core is shown to be liquid-like, revealed by studies of the pair correlation function and structure factor. In Cu, the cascade lifetime is shown to vary from a low of 1 ps for 5 keV cascades to 5 ps for 25 keV cascades [16]. Below 5 keV, no discernible liquid zone can be identified. It is interesting to note that low energy displacements in SiC occur in less than 0.1 ps, which is at least one order of magnitude faster than in metals. This is a consequence of the much stiffer interaction potential in SiC. The issue of cascade lifetime is important, because it has a direct effect on the ability of the cascade to form defect clusters before the collisional phase is over.

In standard dpa calculations, the atomic structure of the collision cascade is irrelevant. However, all evidence suggest that the RCS mechanism is effective in producing surviving single defects (SSD) in metals only in a small shell at the periphery of the cascade. At the core, however, the separation of Frenkel pairs is short-lived because of the molten structure, and the majority either recombine or form clusters. As the cascade size increases, the fraction of SSD will decrease because of the relative decrease of the ratio of the RCS length to cascade size. Instead, the fraction of surviving clustered defects (SCD) increases with PKA energy, because of increased elastic strain energy within the cascade volume. Fig. 4 shows the spatial distribution of atomic

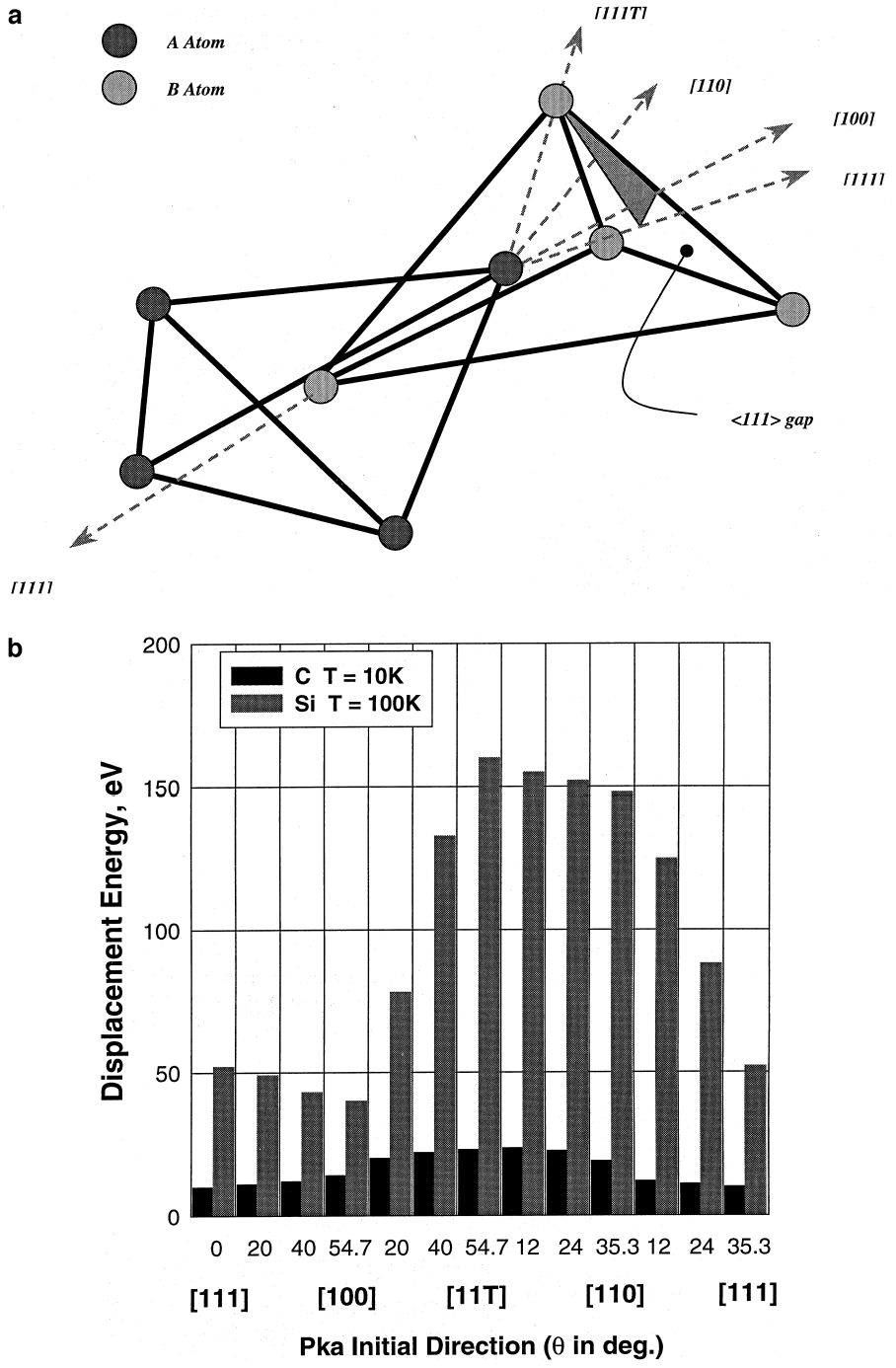

Fig. 3. (a) Primitive cells in SiC, showing displacement directions, (b) Directional dependence of the displacement threshold in SiC.

defects in a 25 keV cascade in Cu after 10 ps [16]. It is clear that a small vacancy cluster has formed at the center, and few smaller interstitial clusters are at the periphery. The exact clustering mechanism is not well established yet. Calculations of atomic level stresses in Au indicate that excessively large compressive stresses exist at the periphery, while high tensile stresses occur at the center [16]. It is therefore tempting to interpret the results of clustering as a consequence of the elastic interaction between self-interstitials, on the one hand, and

between vacancies, on the other. Direct nucleation of interstitial loops in cascades has important consequences on damage accumulation, because it can lead to a production asymmetry between freely migrating vacancies and interstitials, as proposed by Woo and Singh [18]. If this *production bias* is inherent in cascade damage, the *absorption bias* of dislocations for interstitials would not be a pre-requisite for void swelling.

Instead of RCS's emanating from a molten core, atomic displacements in covalent materials are produced in close proximity (within a neighboring primitive cell), because of a strong covalent bond. In silicon, MD simulations for B and As ions with incident energies from 1 to 15 keV have been simulated by Caturla et al. [19]. They observed that for heavy ions, the number of displaced atoms is approximately a factor of two higher than that predicted by the KP model – a surprising result. On the other hand, for light ions, their MD simulations agree with the simple KP model. One interesting feature of damage in Si is that cascades produce amorphous zones (or pockets), that are highly defected. Thus, the standard metal concept of the cascade does not apply here, since the apparent high defect concentration is rather unstable because of the close proximity of defects. In fact, studies of the annealing behavior of amorphous pockets showed that they are readily dissolved, leaving behind a recrystalized region with few atomic defects. At 1080 K, complete recrystalization has taken place by 0.1 ns, for a damage zone produced by a 25-keV cascades in Si [16]. The fraction of isolated atomic defects that are not contained in the amorphous zones is estimated at 10% for heavy ions in Si, and at 30% for light ions. Thus, it appears that at moderate temperatures in Si (e.g. 600 K), the fraction of single defects from cascades is similar to the case of metals.

In BCC metals, such as Fe and V, the general behavior of the cascade is similar to the FCC case, with some additional complications. Recent MD [16] of

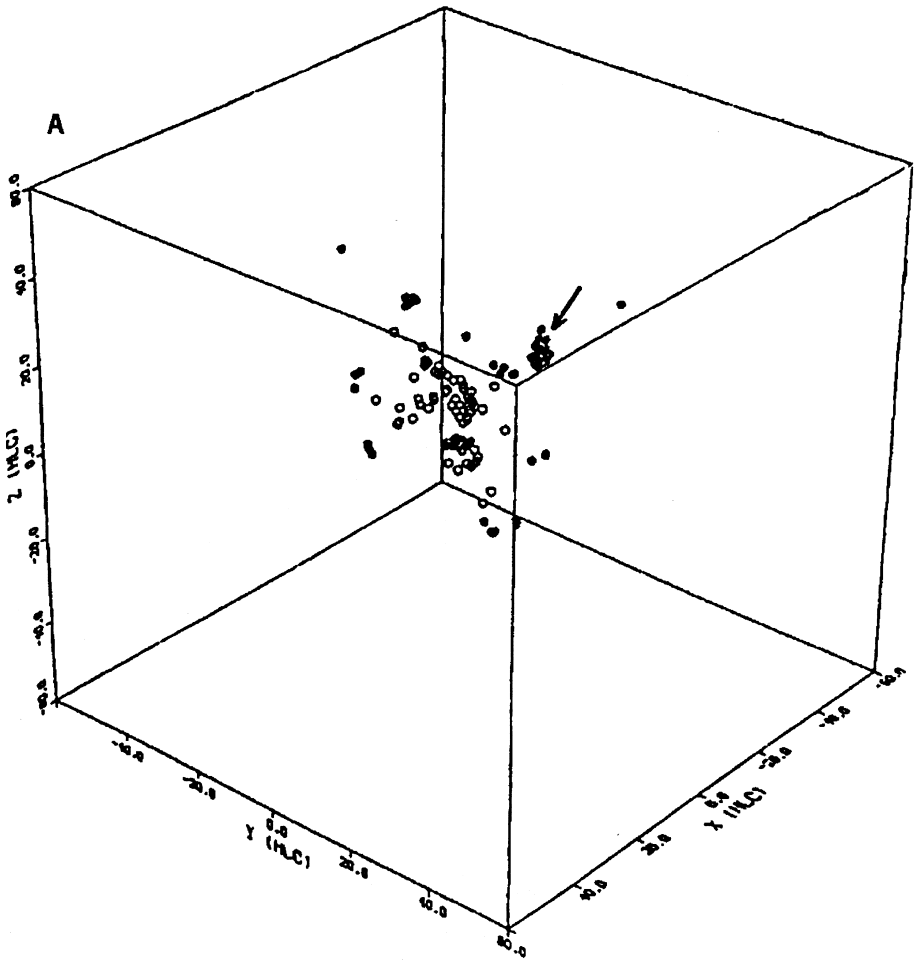

Fig. 4. Cascade structure of a 25 keV Cu PKA, showing clustering of vacancies at the core, and interstitials at the periphery [16].

cascades in BCC Fe showed that the general dependence of the fraction of surviving defects on PKA energy is similar to FCC metals (see Fig. 5). However, no vacancy clusters were produced at the cascade core of either Fe or V, in sharp contrast to studies of Cu and Au. In addition, it is found that only small interstitial loops nucleate within the cascade volume. Once nucleated, di- and tri-interstitial loops glide very quickly along ⟨1 1 1⟩ directions. The activation energy for their migration is estimated as 0.2, 0.067 and 0.17 eV for mono-, di- and tri-interstitials, respectively. The role of the high stacking fault energy on unfaulting glissile loops has not been assessed, and it is uncertain as to the size limit for the mobility of nucleated loops.

4. Damage accumulation

The process of damage accumulation involves the following: (1) inter-cascade interactions, (2) intra-cascade interactions, (3) diffusional migration of FMD. The last item, however, can be conveniently included with microstructure evolution processes, and will therefore not be dealt with here. Within one single cascade, the fraction of surviving defects (SD) is strongly dependent on the PKA energy. This fraction, χ, will be defined as the *defect production efficiency* by the equation: $v_{SD} = \chi K \xi(E) v_{KP}$. Fig. 5 shows the results of several MD simulations of cascades for χ, up to 20 keV, together with experimental resistivity change data. These results indicate that even for one cascade, χ is on the order of 20–30% of the NRT value, for cascade energies above a few keV.

The traditional model of damage accumulation is due to Makin and Minter [4], in which production of cascades is independent of irradiation time, till cascades start to "feel" one another through geometric proximity. At this point, non-linearities set in, and one cascade can partially "heal" the damage of a previous one giving rise to saturation in the density of damage zones. Recently, a

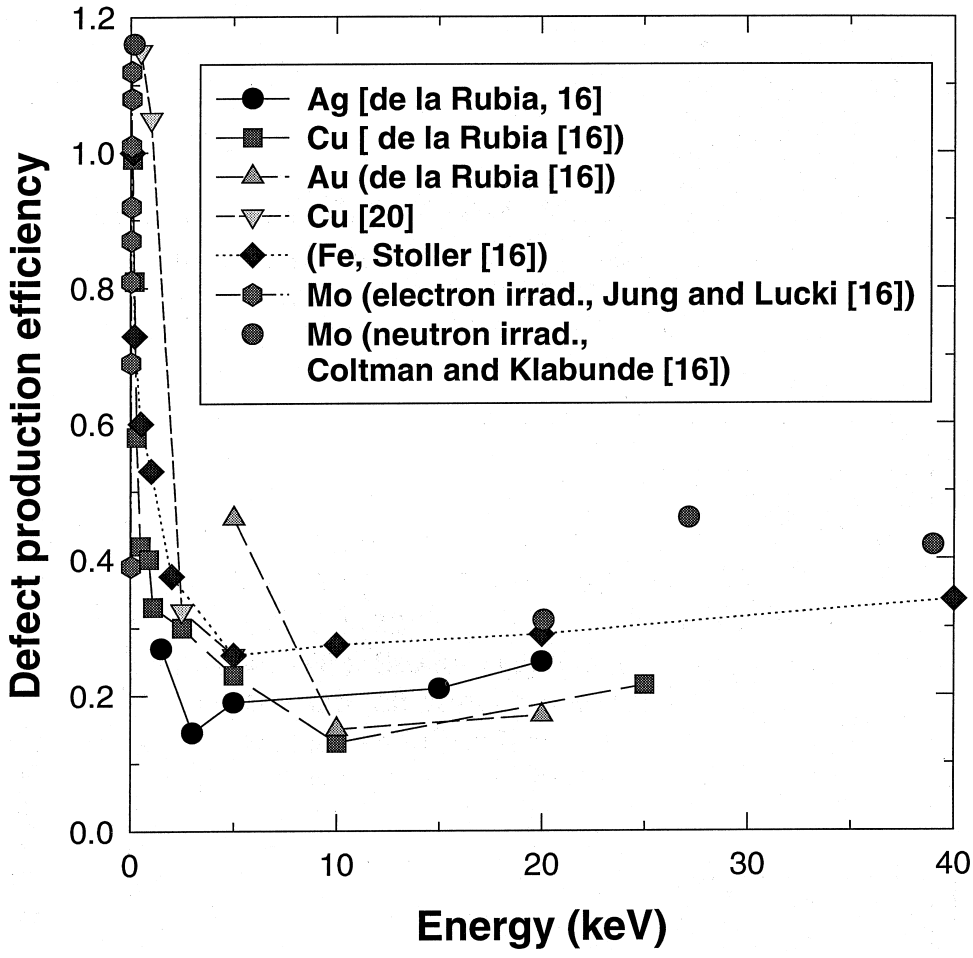

Fig. 5. Defect production efficiency as a function of PKA energy – MD and experiment [15,16,20].

number of investigations [21] showed that this is indeed the case with ion irradiation of Au, except for two new features. First, a group of clusters (e.g. sub-cascades) was identified to occur closely spaced, and was associated with one ion. Second, the irradiation temperature was observed to have a significant effect on the survival of vacancy clusters. The data shows that clusters tended to agglomerate in single zones at high temperatures. Thus, the effect of temperature is to decimate the smaller clusters, and to consolidate them into larger ones. The production efficiency, defined as the ratio of damage clusters per incident ion, was found to decrease from a high of 40% at the beginning of irradiation to less than 10% by an ion fluence of 10^{15} ions/cm^2 at 300 K. The annihilation efficiency was found to increase until it matched the production efficiency at saturation.

The exact mechanism of vacancy cluster collapse into a stacking fault tetrahedron (STF) is not well established. Experimental data show that the density of vacancy clusters increases at a "super-linear" initial rate. This is interpreted as indicative of increased defect production efficiency with neutron fluence – a result that is diametrically opposite to the ion irradiation results of Kanzaki. The data is interpreted in terms of a "shock wave" generated by one cascade and interacting with an existing loose vacancy cluster from a previous one. The pressure wave is thought to result in complete collapse of the cluster into a SFT. The exact details of this proposed mechanism have not been theoretically worked out, and it therefore remains as speculation.

One final area of large uncertainty is the question of the imbalance between vacancies and interstitials in FMD's. Single and multiple free defects diffuse and glide in one dimension over time scales on the order of ms–months, and cover distances that are 3–4 orders of magnitude larger than the cascade volume. The ratio of V/I reacting with microstructural features – the sink bias – is still a matter of debate. The asymmetry in the FMD was originally proposed by Woo and Singh [18] and has recently been shown to result from the formation of I-loops at the cascade periphery by MD simulations. Another mechanism for this asymmetry has been proposed by Kiritani [14], as the Cascade Localization Induced Bias (CLIB) effect. Based on experimental evidence for the disappearance of I-loops under neutron irradiation, it is proposed that the delayed outward migration of vacancies from the cascade core results in their interaction with nucleated I-loops at the periphery.

5. Conclusions

Significant advances in our understanding of damage production and accumulation have been made over the past five decades, albeit at a slow rate. The fundamental picture of displacement damage in collision cascades is well understood. However, many important details remain in a state of complete flux. While the magnitude of the displacement threshold in metals, and the associated RCS mechanism are both developed, this is not the case for many covalent materials. The fraction of displaced atoms surviving a single cascade is now understood to be small ($\sim$0.2). However, the exact split within this fraction of free versus clustered defects is still being debated. A very consistent description of damage production has emerged through theory, computer simulation and experiment. Some of the salient successes are: measurements and calculations of the displacement threshold, nucleation and migration of interstitial loops in cascades, clustering of vacancies at the core of the cascade, the RCS mechanism in metals and the "gap" mechanism in covalent materials, amorphization in covalent materials, and the thermal spike concept in metals.

With all these successes, it may seem that not much is needed for further elaboration. This is emphatically not the case, because many important details remain unsolved. The clustering mechanisms of vacancies and interstitials within the lifetime of a single cascade are not clear. Non-linear inter- and intra-cascade interactions are not very well understood. Experimental evidence range from a "reinforcement" to a "mutual destruction" effect, presumably dependent on fluence, material and temperature. Beyond the single cascade concept, the situation becomes extremely complex. The biggest problem now is how to quantify residual damage accumulation. It is well known that damage is evidenced by microstructure evolution, and not by the number of displaced atoms. The small fraction of defects that did not cluster within one cascade will interact with damage zones of other cascades. Therefore, there is no straightforward way in which the determination of damage accumulation can be generalized, for the purpose of experimental correlations. For a recent review, please see Zinkle and Singh [21]. The accepted dpa measure of damage accumulation can be completely misleading, because it overlooks the important "healing" power of the crystal lattice. Theory and simulation have not yet provided unequivocal answers to many of these questions, because of the vast computational needs of large, interacting cascades with realistic interatomic potentials.

Acknowledgements

The author would like to acknowledge the Department of Energy, Office of Fusion Energy (DOE/OFE) for partial financial support of this research, and LLNL/MRI for additional partial support. Discussions with Drs. de la Rubia and Huang (LLNL), Dr. Singh (Risø) and Dr. Zinkle (ORNL) were very helpful during the course of manuscript preparation. The useful comments

and additional references provided by one of the reviewers are greatly appreciated.

References

[1] G.H. Kinchin, R.S. Pease, Rep. Progr. Phys. 18 (1955) 1.
[2] J.A. Brinkman, J. Appl. Phys. 25 (1954) 961.
[3] A. Seeger, in: Proceedings of the Second United Nations International Conference on the Peaceful Uses of Atomic Energy, Geneva, vol. 6, New York, 1958, p. 250.
[4] M.J. Makin, F.J. Minter, Acta Met. 8 (1960) 691.
[5] P.S. Chou, N.M. Ghoniem, Nucl. Instr. and Meth. B 28 (1987) 175.
[6] J.F. Ziegler, J.P. Biersack, U. Littmark, The Stopping and Range of Ions in Solids, Pergamon, New York, 1985, p. 48.
[7] S.P. Chou, N.M. Ghoniem, Phys. Rev. B 43 (4) (1991) 2490.
[8] M.S. Daw, M.I. Baskes, Phys. Rev. Lett. 50 (1983) 1285.
[9] F.H. Stillinger, T.A. Weber, Phys. Rev. B 31 (1985) 5262.
[10] J. Tersoff, Phys. Rev. Lett. 56 (1986) 632.
[11] H. Huang, N. Ghoniem, J. Nucl. Mater. 199 (1993) 221.
[12] M.T. Robinson, I.M. Torrens, Phys. Rev. B 9 (1974) 5008.
[13] H.L. Heinisch, J. Nucl. Mater. 103&104 (1981) 1325; H. Heinisch, B.N. Singh, Philos. Mag. A67 (1993) 40; Y. Satoh, T. Yosheiie, M. Kiritani, J. Nucl. Mater. 191 (1992) 1101.
[14] M. Kiritani, J. Nucl. Mater. 179–181 (1991) 81; M. Kiritani, J. Nucl. Mater. 155–157 (1988) 113.
[15] C.A. English, M.L. Jenkins, Mater. Sci. Forum 15–18 (1987) 1003.
[16] Phythian, R. Stoller, A.J.E. Foreman, J. Nucl. Mater. 223 (1995) 245; T. Diaz de la Rubia, Annu. Rev. Mater. Sci. 26 (1996) 613; R.E. Stoller, Mat. Res. Soc. Symp. Proc. 373 (1995) 21; R.E. Stoller et al., J. Nucl. Mater. 252 (1997) 49.
[17] S.P. Chou, N.M. Ghoniem, J. Nucl. Mater. 179–181 (1991) 909.
[18] C.H. Woo, B.N. Singh, Philos. Mag. A 65 (1992) 889; B.N. Singh, C.H. Woo, A.J.E. Foreman, Mater. Sci. Forum 97–99 (1992) 75; B.N. Singh, A.J.E. Foreman, Philos. Mag. A 66 (1992) 975.
[19] M.J. Caturla, T. Diaz de la Rubia, L.A. Marques, G.H. Gilmer, Phys. Rev. B 54 (23) (1996) 16683.
[20] N.W. Guinan, J.H. Kinney, J. Nucl. Mater. 103&104 (1981) 1319; F. Gao, S.J. Wooding, A. Calder, D.J. Bacon, Mater. Res. Soc. Symp. Proc. 15 (1995) 373.
[21] D. Bacon et al., J. Nucl. Mater. 151 (1997) 1; S. Zinkle, B.N. Singh, J. Nucl. Mater. 199 (1993) 173; Y. Kanzaki, N. Sekimura, S. Ishino, J. Nucl. Mater. 191–194 (1992) 1119.